UNIVERSITY OF AMSTERDAM

UvA-DARE (Digital Academic Repository)

Role of nuclear receptor Nur77 during inflammation

Hamers, A.A.J.

[Link to publication](#)

CHAPTER 3

Limited Role of
Nuclear Receptor Nur77 in
Escherichia coli-induced
Peritonitis

Limited Role of Nuclear Receptor Nur77 in *Escherichia coli*-Induced Peritonitis

Anouk A. J. Hamers,[a] Sven Uleman,[a] Claudia M. van Tiel,[a] Daniëlle Kruijswijk,[b] Anne-Marieke van Stalborch,[c] Stephan Huveneers,[c] Carlie J. M. de Vries,[a] Cornelis van 't Veer[b]

Department of Medical Biochemistry, Academic Medical Center, University of Amsterdam, Amsterdam, The Netherlands[a]; Center for Experimental and Molecular Medicine, Academic Medical Center, University of Amsterdam, Amsterdam, The Netherlands[b]; Department of Molecular Cell Biology, Sanquin Research and Swammerdam Institute for Life Sciences, University of Amsterdam, Amsterdam, The Netherlands[c]

Nuclear receptor Nur77 (NR4A1, TR3, or NGFI-B) has been shown to play an anti-inflammatory role in macrophages, which have a crucial function in defense against peritonitis. The function of Nur77 in *Escherichia coli*-induced peritoneal sepsis has not yet been investigated. Wild-type and Nur77-knockout mice were inoculated with *E. coli*, and bacterial outgrowth, cell recruitment, cytokine profiles, and tissue damage were investigated. We found only a minor transient decrease in bacterial loads in lung and liver of Nur77-knockout compared to wild-type mice at 14 h postinfection, yet no changes were found in the peritoneal lavage fluid or blood. No differences in inflammatory cytokine levels or neutrophil/macrophage numbers were observed, and bacterial loads were equal in wild-type and Nur77-knockout mice at 20 h postinfection in all body compartments tested. Also, isolated peritoneal macrophages did not show any differences in cytokine expression patterns in response to *E. coli*. In endothelial cells, Nur77 strongly downregulated both protein and mRNA expression of claudin-5, VE-cadherin, occludin, ZO-1, and β-catenin, and accordingly, these genes were upregulated in lungs of Nur77-deficient mice. Functional permeability tests pointed toward a strong role for Nur77 in endothelial barrier function. Indeed, tissue damage in *E. coli*-induced peritonitis was notably modulated by Nur77; liver necrosis and plasma aspartate aminotransferase (ASAT)/alanine aminotransferase (ALAT) levels were lower in Nur77-knockout mice. These data suggest that Nur77 does not play a role in the host response to *E. coli* in the peritoneal and blood compartments. However, Nur77 does modulate bacterial influx into the organs via increased vascular permeability, thereby aggravating distant organ damage.

Peritonitis is an infection caused by bacteria in the normal germfree area of the peritoneal cavity (1). Such an intra-abdominal infection can rapidly turn into life-threatening sepsis, the leading cause of death in critically ill patients in developed countries (2). Peritoneal infection can be caused by multiple bacteria, but *Escherichia coli* is the most commonly found pathogen in cases of peritonitis (60%) (3). Both the host and bacteria may contribute to the development of disease after *E. coli* infections (4). The innate immune system protects the host against bacterial infections by pattern recognition receptors, such as Toll-like receptors (TLRs) and NOD-like receptors (NLRs), that recognize a variety of bacterial components. These receptors then activate signal transduction pathways, which in turn activate latent transcription factors, such as nuclear factor kappa B (NF-κB) and activator protein 1 (AP-1) family members. Upon activation, these transcription factors translocate to the nucleus to induce the expression of a large number of genes that initiate the inflammatory response, e.g., tumor necrosis factor alpha (TNF-α) and cyclooxygenase-2 (COX2), and exert antimicrobial activities by generating reactive oxygen species (ROS). Also, chemokines are produced via this route to attract additional phagocytes to the site of infection, which will engulf and kill the microbes, as well as adaptive immune cells (5). Failure of the immune system to eradicate the bacteria may lead to dissemination of the infection and sepsis (6). When sepsis occurs, the initial peritoneal infection becomes a life-threatening disease, with a mortality rate of up to 80% (7).

Nuclear receptor Nur77, also known as NR4A1, TR3, or NGFI-B, is a member of the NR4A subfamily of nuclear receptors that also comprises Nurr-1 (NR4A2 or NOT) and NOR-1 (NR4A3 or MINOR). Like other nuclear receptors, the NR4As consist of an N-terminal transactivation domain, a central zinc finger DNA binding domain, and a C-terminal ligand binding domain. So far, no ligands have been identified for the NR4A nuclear receptors, and therefore, they are referred to as orphan nuclear receptors. All three NR4A nuclear receptors can bind as monomers to the NGFI-B response element (NBRE) (AAAGG CTA) of direct target genes. Nur77 and Nurr1 can also form homodimers and heterodimers with retinoid X receptor and bind a DR-5 response element (8, 9). Induction of Nur77 can be achieved upon stimulation with inflammatory factors such as prostaglandins, TNF-α, lipopolysaccharide (LPS), gamma interferon (IFN-γ), and granulocyte-macrophage colony-stimulating factor (GM-CSF) (10–12). It has been shown in RAW264.7 macrophages that Nur77 potentiates LPS-induced expression of myristoylated alanine-rich protein kinase C substrate (MARCKS), NF-κB-inducing kinase (NIK), IκB kinase epsilon (IKKi), and cyclin D2, and based on these data, it was concluded that Nur77 is a proinflammatory nuclear receptor (13). In that study, it was also demonstrated that the expression of these specific genes in peritoneal macrophages derived from wild-type (WT) and Nur77-knockout (Nur77$^{-/-}$) mice was not different after LPS stimulation, indicating that these genes may not be optimal to monitor Nur77-medi-

ated macrophage phenotypic changes. We demonstrated that overexpression of this receptor in human THP-1 macrophages reduces the expression of several inflammatory cytokines in response to either LPS or TNF-α (10). Furthermore, knockdown of Nur77 in THP-1 macrophages resulted in increased inflammatory gene expression. It has been proposed that Nur77 modulates inflammatory gene expression at least in part through transrepression of NF-κB, in line with studies showing that Nur77 inhibits NF-κB activity by binding its p65 subunit (14, 15).

In line with our previous findings, Nur77$^{-/-}$ bone marrow-derived macrophages (16) and peritoneal macrophages (17) display a more proinflammatory phenotype after LPS stimulation. In that same study, we showed that thioglycolate-induced migration of circulating cells to the peritoneal cavity was markedly increased in Nur77$^{-/-}$ mice. In atherosclerosis bone marrow, specific deletion of Nur77 aggravates the disease, with vascular lesions containing more macrophages, T cells, and chemokine SDF-1α (16, 17). Of note, it was also recently described that Nur77 does not affect atherosclerosis (18). Hanna et al. (19) demonstrated that Nur77$^{-/-}$ mice lack the patrolling Ly6C^{lo} monocyte population in bone marrow, spleen, and blood.

The function of Nur77 in an acute-infection model of *E. coli*-induced peritonitis has not yet been investigated and was the subject of the current study. Therefore, we inoculated WT and Nur77$^{-/-}$ mice with *E. coli* bacteria and investigated bacterial outgrowth, cell recruitment, cytokine profiles, and tissue damage. Deficiency of Nur77 did not play a role in the host response to *E. coli* regarding the peritoneal and blood compartments; however, Nur77 does protect from distant organ damage.

MATERIALS AND METHODS

Mice. Nur77$^{-/-}$ mice (20) on a C57BL/6.J background were kindly provided by B. R. Binder (Vienna, Austria). WT mice with a C57BL/6.J background were obtained from Jackson Laboratories. The Nur77$^{-/-}$ mice were backcrossed with WT mice and kept by in-house breeding. The animals had a conventional microbiological status and were housed in individually ventilated cage racks (4 mice/cage). Mice were fed a chow diet and acidified water, *ad libitum*. All animal experiments were approved by the Committee for Animal Welfare of the Amsterdam Medical Center and were carried out in compliance with guidelines issued by the Dutch government.

Induction of *E. coli* peritonitis. Peritonitis was induced as described previously (21). In brief, *E. coli* strain O18:K1 bacteria were cultured in Luria-Bertani (LB) medium (Difco) at 37°C to mid-log phase and washed twice with pyrogen-free sterile 0.9% NaCl (Baxter, Lessines, Belgium) before inoculation. The amount of bacteria was determined by measuring the A_{600} with a spectrophotometer. WT and Nur77$^{-/-}$ mice ($n = 8$; both sexes; 10 to 12 weeks old) were injected with 1×10^4 CFU in 200 μl of pyrogen-free saline. The inoculum was plated onto blood agar plates in serial dilutions to verify the amount of viable bacteria injected.

Collection of samples after induction of peritonitis. After 0, 6, 14, and 20 h, mice were sacrificed under inhalation anesthesia with isoflurane. Peritoneal lavage was performed with 5 ml of sterile phosphate-buffered saline (PBS) using an 18-gauge needle. The peritoneal lavage fluid (PLF) was collected into sterile tubes and placed on ice. Next, blood was drawn by heart puncture, collected into sterile tubes containing heparin, and immediately placed on ice. Subsequently, the abdomen was opened, and liver and lungs were harvested and divided. Liver and lung samples were weighed, 4 volumes of PBS was added, and these samples were homogenized by using a tissue homogenizer (Biospec Products). Other liver and lung samples were fixed in 4% formalin and embedded in paraffin for histological analysis. Additionally, liver samples were snap-frozen in liquid nitrogen and stored at −80°C.

Determination of bacterial loads in the PLF, blood, liver, and lung. To determine the amount of bacteria, the PLF, blood, and liver and lung homogenates were plated in serial dilutions onto blood agar plates overnight at 37°C. The numbers of CFU were counted.

Assays. Five volumes of Greenburger lysis buffer (150 mM NaCl, 15 mM Tris, 1 mM MgCl · H$_2$O, 1 mM CaCl$_2$, 1% Triton [Sigma-Aldrich]) was added to the lung homogenates, the samples were incubated for 20 min, and an enzyme-linked immunosorbent assay (ELISA) for myeloperoxidase (MPO; R&D systems) was performed on the supernatants according to the manufacturer's instructions. Interleukin-6 (IL-6), IL-10, monocyte chemotactic protein 1 (MCP-1), IFN-γ, and TNF-α levels were measured by using the Cytometric Bead Array Mouse Inflammation kit (BD Biosciences), according to the manufacturer's instructions. The levels of keratinocyte receptor/chemokine ligand 1 (KC/CXCL1) and E-selectin were detected by ELISA using Duo-Set antibodies according to the manufacturer's instructions (R&D Systems, Abington, United Kingdom). Aspartate aminotransferase (ASAT), alanine aminotransferase (ALAT), and lactate dehydrogenase (LDH) were detected with commercially available kits (Sigma-Aldrich) by using a Hitachi analyzer (Roche) according to the manufacturer's instructions.

White blood cell counts and differentials. The number of cells in the PLF was determined by the addition of Zap-oglobulin and subsequent counting of cell nuclei with a Coulter Counter (Beckman, Miami, FL). Cytospin preparations were stained with Grünwald-Giemsa stain (Diff-Quick) and were quantified by manual differential cell counting.

Immunohistochemistry. Paraffin sections of lung and liver were deparaffinized and rehydrated. To detect macrophages in the liver (F4/80; SBA), the sections were incubated in 1% (vol/vol) hydrogen peroxide (Merck), followed by antigen retrieval at pH 6.0. The sections were blocked with Ultra-V-Block (Thermo Scientific) and were subsequently incubated with the first antibody overnight at 4°C, followed by a horseradish peroxidase (HRP)-conjugated secondary rabbit anti-rat antibody (Immunologic). To detect neutrophils in lung and liver (Ly6G; Serotec), no antigen retrieval was necessary. The sections were blocked by using 1% (vol/vol) normal goat serum and 1% (wt/vol) bovine serum albumin (BSA) in Tris-buffered saline (TBS). The first antibody was incubated for 1 h at room temperature, followed by an HRP-conjugated secondary donkey anti-rat antibody (Jackson Laboratories).

Apoptotic cells were detected with an antibody against cleaved caspase-3 (Thermo Scientific), antigen retrieval was performed at pH 6.0, and sections were blocked with Ultra-V-Block (Thermo Scientific). The first antibody was incubated overnight at 4°C, followed by a poly-HRP-conjugated secondary goat anti-rabbit antibody (Powervision). For every staining, 3,3′-diaminobenzidine (DAB) substrate (Immunologic) was used for detection. After counterstaining with hematoxylin, sections were embedded in Pertex (HistoLab). The stainings were quantified by counting the number of cells manually in 5 areas/section (1 section/mouse).

Pathology. To score liver and lung injury, 7-μm sections were stained with hematoxylin-eosin (Sigma-Aldrich), and injury was scored in a blind fashion by a pathologist. For liver injury, interstitial inflammation, formation of thrombi, and hepatocellular necrosis were scored. Lung injury was scored for the following parameters: interstitial inflammation, edema, pleuritis, and thrombus formation. Each parameter was scored on a scale of 0 to 4 as follows: 0 for no injury, 1 for mild injury, 2 for moderate injury, 3 for severe injury, and 4 for very severe injury. The total injury score was expressed as the sum of all parameters scored, with a maximum score of 16.

***Ex vivo* peritoneal macrophage stimulation.** Peritoneal lavage cells were obtained by flushing the peritoneal cavity with ice-cold sterile PBS as described above. Peritoneal cells were washed, counted, resuspended in RPMI 1640 medium (Invitrogen) containing 10% fetal calf serum (FCS; Gibco) and penicillin-streptomycin (culture medium) at a concentration of 1×10^6 cells/ml, and incubated for 2 h at a density of 10^5 cells/well in a 96-well culture plate (Greiner, Alphen aan den Rijn, The Netherlands). Thereafter, adherent macrophages were washed with culture medium to

TABLE 1 Primer sequences used for semiquantitative real-time PCR

Gene	Forward primer sequence	Reverse primer sequence
36B4	5′-GGACCCGAGAAGACCTCCTT-3′	5′-GCACATCACTCAGAATTTCAATGG-3′
Nur77	5′-GGATGAGGGAAGTGAGAAGATTGG-3′	5′-ACAAGAGGCGGCGGAACC-3′
TNF-α	5′-AGATAGCAAATCGGCTGACG-3′	5′-AGCGCATGGATCTCAAAGAC-3′
IL-6	5′-GTTCTCTGGGAAATCGTTGGA-3′	5′-GGAAATTGGGGTAGGAAGGA-3′
IL-1β	5′-GCAACTGTTCCTGAACTCAACT-3′	5′-ATCTTTTGGGGTCCGTCAACT-3′
MCP-1	5′-AGCACCAGCCAACTCTCACT-3′	5′-CGTTAACTGCATCTGGCTGA-3′
RANTES	5′-TCGTGCCCACGTCAAGGAGTATTT-3′	5′-TCTTCTCTGGGTTGGCACACACTT-3′
MIP-2	5′-GCCAAGGGTTGACTTCAAGA-3′	5′-TTCAGGGTCAAGGCAAACTT-3′
SOCS-1	5′-GACACTCACTTCCGCACCTT-3′	5′-AAGAAGCAGTTCCGTTGGC-3′
A20	5′-GGGACTCCAGAAACAAGGG-3′	5′-TACCCTTCAAAACATGGTGCTT-3′
IRAK-M	5′-TGCCAGAAGAATACATCAGACAG-3′	5′-TCTAAGAAGGACAGGCAGGAGT-3′
P0[a]	5′-TCGACAATGGCAGCATCTAC-3′	5′-ATCCGTCTCCACAGACAAGG-3′
Nur77[a]	5′-GTTCTCGGAGGTCATCCGCAAG-3′	5′-GCAGGGACCTTGAGAAGGCCA-3′
Claudin-5[a]	5′-CTCTGCTGGTTCGCCAACAT-3′	5′-CAGCTCGTACTTCTGCGACA-3′
VE-cadherin[a]	5′-AAGCGTGAGTCGCAAGAATG-3′	5′-TCTCCAGGTTTTCGCCAGTG-3′
Occludin[a]	5′-ACAAGCGGTTTTATCCAGAGTC-3′	5′-GTCATCCACAGGCGAAGTTAAT-3′
β-Catenin[a]	5′-CATCTACACAGTTTGATGCTGCT-3′	5′-GCAGTTTTGTCAGTTCAGGGA-3′
eNOS[a]	5′-TGATGGCGAAGCGAGTGAAG-3′	5′-ACTCATCCATACACAGGACCC-3′
Claudin-5	5′-AGTTAAGGCACGGGTAGCAC-3′	5′-GTACTTCTGTGACACCGGCA-3′
VE-cadherin	5′-TGCAACCTGGATCAGACACC-3′	5′-GGGCCTGGAATTTGCTACCT-3′
Occludin	5-'TTGAAAGTCCACCTCCTTACAGA-3′	5′-CCGGATAAAAAGAGTACGCTGG-3′
β-Catenin	5′-CCCAGTCCTTCACGCAAGAG-3′	5′-CATCTAGCGTCTCAGGGAACA-3′
ZO-1[a]	5′-CAACATACAGTGACGCTTCACA-3′	5′-CACTATTGACGTTTCCCCACTC-3′
ZO-1	5′-GCTTTAGCGAACAGAAGGAGC-3′	5′-TTCATTTTTCCGAGACTTCACCA-3′

[a] Human primers.

remove the nonadherent cells. Next, the cells were stimulated with 10^5 CFU of growth-arrested *E. coli* bacteria, as described previously (21), for 1, 4, 8, and 24 h in culture medium at 37°C and 5% CO_2 in a humidified atmosphere. Cell-free supernatant was harvested for determination of TNF-α, IL-6, and KC levels by ELISA. Total RNA was extracted by using the Aurum Total RNA minikit (Bio-Rad), and cDNA was made with the iScript cDNA synthesis kit (Bio-Rad) for semiquantitative real-time PCR (MyIQ system; Bio-Rad) with 36B4 to correct for cDNA content. Primers used are shown in Table 1.

Lentiviral infection and stimulation of human umbilical vein endothelial cells. Human umbilical vein endothelial cells (HUVECs) were isolated and cultured as previously described (22). Recombinant lentiviral particles encoding Nur77 were produced, concentrated, and titrated as described previously (10). HUVECs were transduced with recombinant lentivirus for 24 h, after which the medium was refreshed, cultured for another 72 h, and stimulated with 10^6 CFU of growth-arrested *E. coli* bacteria for 6 h. Transduction efficiency was determined by immunofluorescence. Cells were harvested, RNA was extracted, and real-time quantitative PCR (qPCR) was performed as described above. Primers used are shown in Table 1.

Immunoblotting. HUVECs were transduced and treated for 24 h with 10^6 CFU of growth-arrested *E. coli* bacteria as described above, after which the cells were washed twice with serum-free M199 medium and lysed in ice-cold NP-40 lysis buffer (50 nM Tris-HCl [pH 7.4], 100 mM NaCl, 10 mM NaF, 1 mM Na_3PO_4, 10% glycerol, 1% Nonidet). After a 10-min incubation on ice, the lysates were collected, sonicated for 1 min, and boiled in sample buffer containing dithiothreitol (DTT). Samples were thereafter analyzed by SDS-PAGE. High-molecular-weight proteins such as zona occludens protein 1 (ZO-1) and VE-cadherin were separated on 7.5% polyacrylamide–SDS gels, and other proteins were separated on 12% gels. Proteins were transferred onto 0.2-μm nitrocellulose membranes (Whatman) by using the Trans-Blot Turbo transfer system (Bio-Rad). The high-molecular-weight proteins were transferred by wet blotting overnight at 4°C. Blots were subsequently blocked in 5% (wt/vol) nonfat milk in TBS and incubated with specific primary antibodies overnight at 4°C, followed by a horseradish peroxidase-labeled secondary an-

tibody (Bio-Rad) for 1 h at room temperature. The following primary antibodies were used: anti-claudin-5 (Zymed), anti-ZO-1 (Invitrogen), anti-β-catenin (Cell Signaling), anti-occludin (Invitrogen), VE-cadherin (Santa Cruz Biotechnology), anti-Nur77 (M210; Santa Cruz Biotechnology), anti-eNOS (Cell Signaling), anti-P-eNOS (Ser^{1177}; Cell Signaling), and α-tubulin (Cedarlane). Proteins were visualized with an enhanced chemiluminescence (ECL) detection system (Thermo Scientific), and quantification of signals was performed by using intensity measurements in ImageJ software.

Immunofluorescence. HUVECs were cultured on fibronectin-coated glass coverslips and transduced with mock or Nur77 lentivirus. After treatment, the cells were washed twice with serum-free M199 and fixed with 4% Formalfix for 20 min. PBS was used as the incubation and wash buffer and was supplemented with 1% (wt/vol) BSA during antibody incubations. Next, cells were permeabilized in PBS containing 0.2% (vol/vol) Triton X-100 for 10 min and blocked with 5% BSA in PBS. Cells were immunostained with anti-Nur77 (M210; Santa Cruz Biotechnology) and secondary anti-mouse AlexaFluor488 (Invitrogen) antibodies and fluorescently labeled anti-VE-cadherin–AlexaFluor647 (BD Biosciences) and phalloidin-AlexaFluor415 (Promokine). Fluorescent imaging was performed by using a Zeiss Axiovert wide-field microscope and a 60× oil objective.

Transwell permeability assay. HUVECs were transduced, trypsinized, and reseeded onto transwells containing a fluorescence-blocking polyethylene terephthalate (PET) track etched membrane with 3-μm pores, separating the upper and lower chambers in 24-well plates (Falcon). After overnight stimulation with 10^6 CFU of growth-arrested *E. coli* bacteria, 1 mg/ml fluorescein isothiocyanate (FITC)-labeled dextran (70 kDa) in HEPES-buffered salt solution (25 mM HEPES, 120 mM NaCl, 5.4 mM KCl, 1.8 mM $CaCl_2$, 25 mM $NaHCO_3$, 15 mM glucose) was added to the upper chamber. After 40 min, total fluorescence in the lower compartment was measured by fluorometry (Novostar).

Electric cell-substrate impedance sensing. Monolayer formation and barrier function were determined by measuring electrical transendothelial resistance (TER) with electric cell-substrate impedance sensing (ECIS). A total of 1.5×10^5 Nur77- or mock-transduced HUVECs were
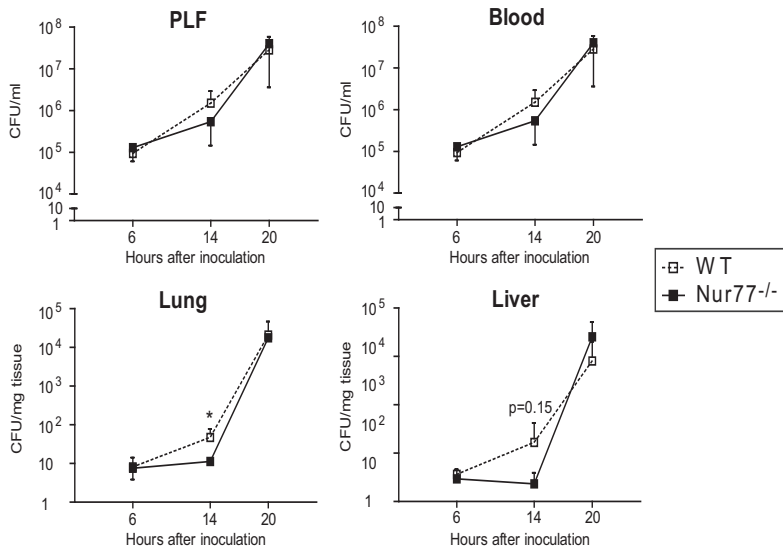
FIG 1 Local and systemic outgrowth of bacteria. Nur77$^{-/-}$ and WT mice were challenged intraperitoneally with 10^4 pathogenic *E. coli* bacteria and sacrificed after 6, 14, and 20 h. Data are means $\pm$ SEM ($n = 8$/group/time point) (*, $P < 0.05$).

seeded onto gold electrode arrays (8W10E; Ibidi, Planegg, Germany) treated with 10 mM L-cysteine (Sigma) for 15 min at 37°C and coated with fibronectin. Measurements were started directly after the cells were seeded, and impedance measurements were performed at 30 kHz.

Statistical analysis. Statistical analysis was performed by using Graph-Pad Prism 5 software. Statistical significance was calculated by using the unpaired Student *t* test. Values are represented as means $\pm$ standard errors of the means (SEM) or standard deviations (SD), as indicated. The significance level was set at a *P* value of <0.05.

RESULTS

Reduced bacterial outgrowth in organs of Nur77$^{-/-}$ mice. To elucidate the role of Nur77 in sepsis, investigations were carried out by using a highly reproducible model of bacterial peritonitis that displays many features of human sepsis (21, 23–25). To obtain a first insight, the bacterial loads at different time points were determined by counting CFU in four body compartments (Fig. 1): the peritoneal cavity, which is the initial site of infection; the blood, to evaluate systemic disease; and lung and liver, organs distant from the primary site of infection. In all body compartments, the CFU increased drastically over time in both WT and Nur77$^{-/-}$ mice. No differences in bacterial loads were found between WT and Nur77$^{-/-}$ mice at 6 h postinfection. However, 14 h after *E. coli* administration, bacterial loads seemed to be lower in the liver and lungs of the Nur77$^{-/-}$ mice, yet this was significant only for the lungs. The bacterial outgrowth in the PLF and blood was not affected by Nur77 deficiency. After 20 h, CFU loads were equal in all compartments of WT and Nur77$^{-/-}$ mice. Overall, Nur77 does not seem to be involved in controlling bacterial outgrowth in PLF and blood. However, Nur77 does show a minor transient effect on bacterial outgrowth in both lung and liver compartments.

Nur77 does not play a pivotal role in cytokine release. Because cytokines are essential mediators of the host response to

infection, we determined levels of the proinflammatory cytokines TNF-α and IL-6, the anti-inflammatory cytokine IL-10, and the chemokine MCP-1 in PLF (Fig. 2A) and blood (Fig. 2B). In the PLF, the levels all cytokines investigated increased over time. Remarkably, no differences in cytokine levels between WT and Nur77$^{-/-}$ mice were found. In blood, the levels of all cytokines first showed an increase from 0 to 6 h postinfection and then a moderate decrease from 6 to 14 h postinfection, and thereafter, the levels increased again. Concentrations of all cytokines measured were similar in WT and Nur77$^{-/-}$ mice. In addition, we measured the levels of the above-mentioned cytokines in the lung homogenates (Fig. 2C) and found no differences between both groups. To assess endothelial cell activation, we investigated (soluble) E-selectin levels in plasma and lung homogenates (Fig. 2D) and observed significantly lower plasma levels in Nur77$^{-/-}$ mice after 6 h of infection. This difference was gone after 14 and 20 h postinfection. In the lung, however, no significant differences between the groups were found. Also, KC levels were studied as a mediator of neutrophil attraction (Fig. 2E). KC levels in the PLF were found to be decreased in Nur77$^{-/-}$ mice 14 h after *E. coli* administration, which may indicate less neutrophil influx into the peritoneal cavity of these mice. In plasma, the KC levels did not differ between both groups. Taken together, Nur77$^{-/-}$ mice displayed decreased levels of soluble E-selectin in plasma and KC in the PLF, yet the concentrations of the inflammatory cytokines tested were not changed.

Nur77 does not mediate neutrophil or macrophage influx. Because neutrophils, macrophages, and lymphocytes play an important role in local host defense against invading bacteria, we next performed cell counts and differentiation of the PLF during peritonitis (Fig. 3A). In response to intraperitoneal administration of 10^4 CFU of *E. coli*, neutrophil numbers increased over time. No significant difference between WT and Nur77$^{-/-}$ mice
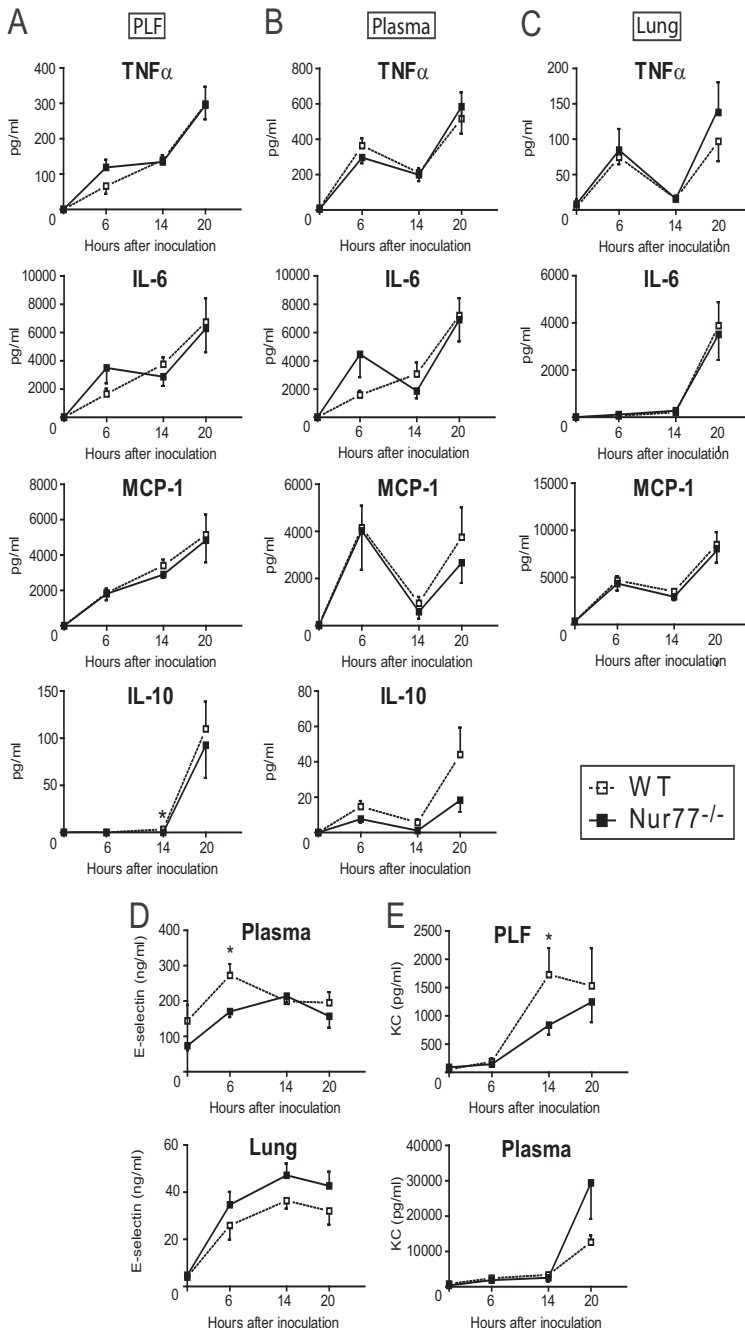
FIG 2 Cytokine/chemokine profiles for peritoneal lavage fluid, plasma, and lung. Nur77$^{-/-}$ and WT mice were challenged intraperitoneally with 10^4 pathogenic *E. coli* bacteria and sacrificed after 0, 6, 14, and 20 h. (A to C) TNF-α, IL-6, MCP-1, and IL-10 levels in PLF (A), plasma (B), and lung (C) were determined. (D and E) E-selectin levels in plasma and lung (D) and KC levels in PLF and plasma (E) were also evaluated. Data are means ± SEM (*n* = 8 mice/group/time point) (∗, *P* < 0.05).
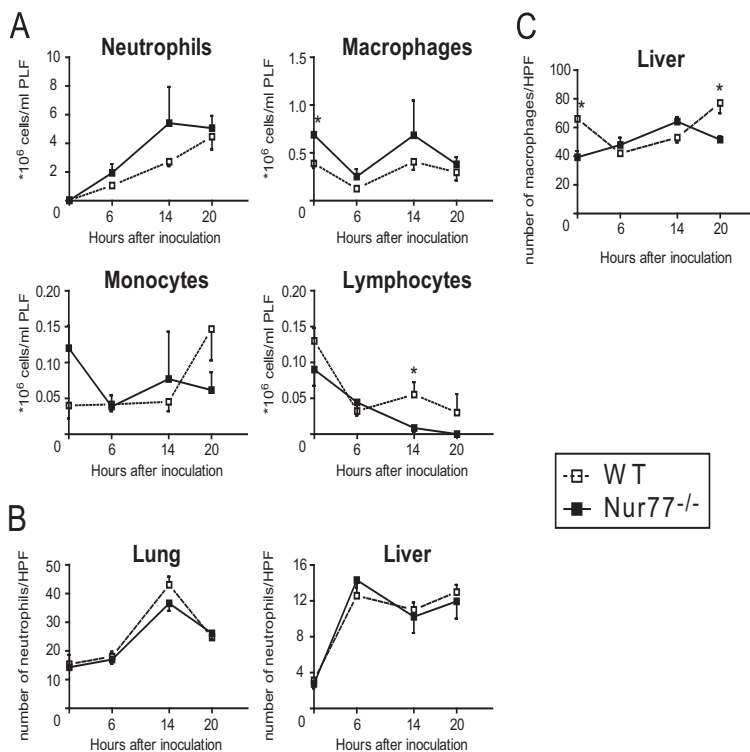
FIG 3 Numbers of inflammatory cells in PLF, lungs, and liver. Nur77$^{-/-}$ and WT mice were challenged intraperitoneally with 10^4 pathogenic *E. coli* bacteria and sacrificed after 0, 6, 14, and 20 h. (A) The amounts of neutrophils, macrophages, monocytes, and lymphocytes in the PLF cytospins were determined. (B and C) Neutrophils (B) and macrophages (C) in the liver were quantified by immunohistochemistry. HPF, high-power field. Data are means ± SEM (*n* = 8 mice/ group/time point) (∗, *P* < 0.05).

was found at any time point, which does not seem to correspond with the lower KC levels found in the PLF of the Nur77$^{-/-}$ mice. The concentration of macrophages present in the PLF decreased from 0 to 6 h and increased from 6 to 14 h; thereafter, these numbers decreased again. The monocyte concentration decreased from 0 to 6 h; thereafter, the influx into the peritoneal cavity of WT mice increased over the time considered, which was not observed in Nur77$^{-/-}$ mice. Macrophage concentrations were significantly higher only in healthy animals, and this difference was gone after infection. However, for monocyte counts, there was no significant difference found between the groups at any of the time points. However, lymphocyte numbers 14 h after *E. coli* administration were significantly lower in Nur77$^{-/-}$ mice than in WT mice. In addition, we determined the numbers of neutrophils (Fig. 3B) and macrophages (Fig. 3C) in lung and liver by immunohistochemistry. Surprisingly, no differences were observed between Nur77$^{-/-}$ and WT mice regarding neutrophil influx into lung or liver. In liver, a significantly lower number of macrophages was found in healthy animals and at 20 h postinfection, while after 6 and 14 h, this was not apparent. Hence, overall neutrophil and macrophage influx was not influenced by Nur77 in all body compartments tested.

Nur77 deficiency protects from organ injury during abdominal sepsis. This model of *E. coli*-induced peritonitis is associated with organ damage (26). To obtain insight into the role of Nur77 during abdominal sepsis, we determined lung and liver damage at 20 h postinfection using hematoxylin-eosin stained sections. Lungs from both WT and Nur77$^{-/-}$ mice showed clear signs of inflammation (Fig. 4A). Total histology scores were similar for both groups. When the individual aspects of the pathology score (inflammation, edema, and thrombi) were examined, there were no significant differences observed between WT and Nur77$^{-/-}$ mice. However, the incidences of thrombi in Nur77$^{-/-}$ and WT lungs were 0% and 37.5% (3 out of 8 mice), respectively. Both WT and Nur77$^{-/-}$ mice also showed signs of liver inflammation (Fig. 4B). The extent of total injury was similar in both groups. However, the Nur77$^{-/-}$ mice showed a significant decease in necrosis. This result was confirmed by clinical chemistry showing clearly diminished ALAT and ASAT levels in the plasma of Nur77$^{-/-}$ mice (Fig. 4C). We measured LDH levels to investigate overall tissue damage and found a trend similar to that found for ASAT and ALAT, yet this was not significant. In addition, at 6 h postinfection, the number of cells positive for cleaved caspase-3, an early marker for apoptosis and, thus, tissue damage, was significantly lower in lungs and livers of Nur77$^{-/-}$ mice (Fig. 4D). Taken together, these data indicate that Nur77 does play a major role in the severity of organ damage induced by abdominal sepsis.
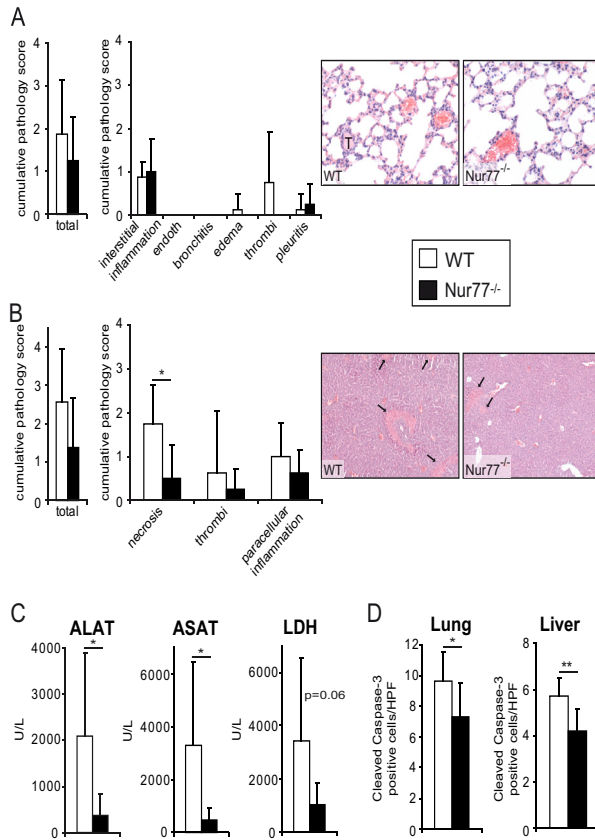
FIG 4 Impact of Nur77 on distant organ injury. Nur77$^{-/-}$ and WT mice were challenged intraperitoneally with 10^4 pathogenic *E. coli* bacteria and sacrificed after 6 h (D) and 20 h (A to C). (A and B) Lung (A) and liver (B) pathology was scored on hematoxylin-eosin-stained, formaldehyde-fixed paraffin sections at 20 h. Original magnifications, ×200 (lung) and ×50 (liver). "T" indicates a thrombus, and the arrows indicate areas of necrosis. (C) Plasma concentrations of ALAT, ASAT, and LDH are also shown. (D) Cleaved caspase-3 immunohistochemistry was quantified at 6 h. Data are means ± SD (*n* = 8 mice/group/time point) (∗, *P* < 0.05; ∗∗, *P* < 0.01).

Nur77 does not play a role in responsiveness of peritoneal macrophages to *E. coli*. To elucidate whether Nur77$^{-/-}$ peritoneal macrophages are more proinflammatory than WT cells, similar to previously reported data on bone marrow-derived macrophages, we investigated the *in vitro* response of these macrophages to *E. coli* O18: K1. We employed growth-arrested bacteria to determine the contribution of Nur77 to the response to a fixed number of intact *E. coli* bacteria over time (Fig. 5). As expected, in the WT cells, the Nur77 mRNA level increased over time upon exposure to 10^5 intact *E. coli* bacteria and decreased again after 4 h of stimulation (Fig. 5A). Also, Nur77 was not expressed in deficient cells. Both WT and Nur77$^{-/-}$ macrophages showed induction of mRNA expression of TNF-α, IL-6, and IL-1β upon *E. coli* stimulation (Fig. 5A). However, Nur77 deficiency did not influence these expression patterns. Expression of the chemokines MCP-1, RANTES, and MIP-2 were also not affected by Nur77 deficiency. mRNA expression of the TLR inhibitors SOCS-1, A20, and IRAK-M was also induced by *E. coli* and similarly in WT and Nur77$^{-/-}$ peritoneal macrophages. Both WT and Nur77$^{-/-}$ macrophages showed similar release patterns of TNF-α, IL-6, and KC after stimulation. Taken together, these data showed that Nur77 did not play a role in the inflammatory response of peritoneal macrophages to *E. coli* bacteria.

Nur77 influences endothelial barrier function. Nur77 is known to play a role in endothelial cell function (27–29), and as we did not find a clear effect on macrophages in the sepsis model, we investigated the role of Nur77 in tight and adherens junction formation in HUVECs (Fig. 6). After stimulating freshly isolated HUVECs with 10^6 growth-arrested *E. coli* bacteria, we observed an increase in Nur77 mRNA levels within 1 h (Fig. 6A). Subsequently, we ectopically increased the expression of Nur77 in HUVECs and found that Nur77 strongly downregulates claudin-5, VE-cadherin, occludin, ZO-1, and, to a lesser extent, β-catenin mRNA expression in these cells, indicating that Nur77 regulates monolayer integrity of the endothelium and, thus, vascular permeability (Fig. 6B). This result was partially confirmed by mRNA expression in the lungs of healthy WT and Nur77$^{-/-}$ mice, showing increases in claudin-5, occludin, and β-catenin mRNA levels. However, there was no detectable difference between WT and Nur77$^{-/-}$ mice in VE-cadherin and ZO-1 expression levels in lung. Furthermore, we found decreased en-
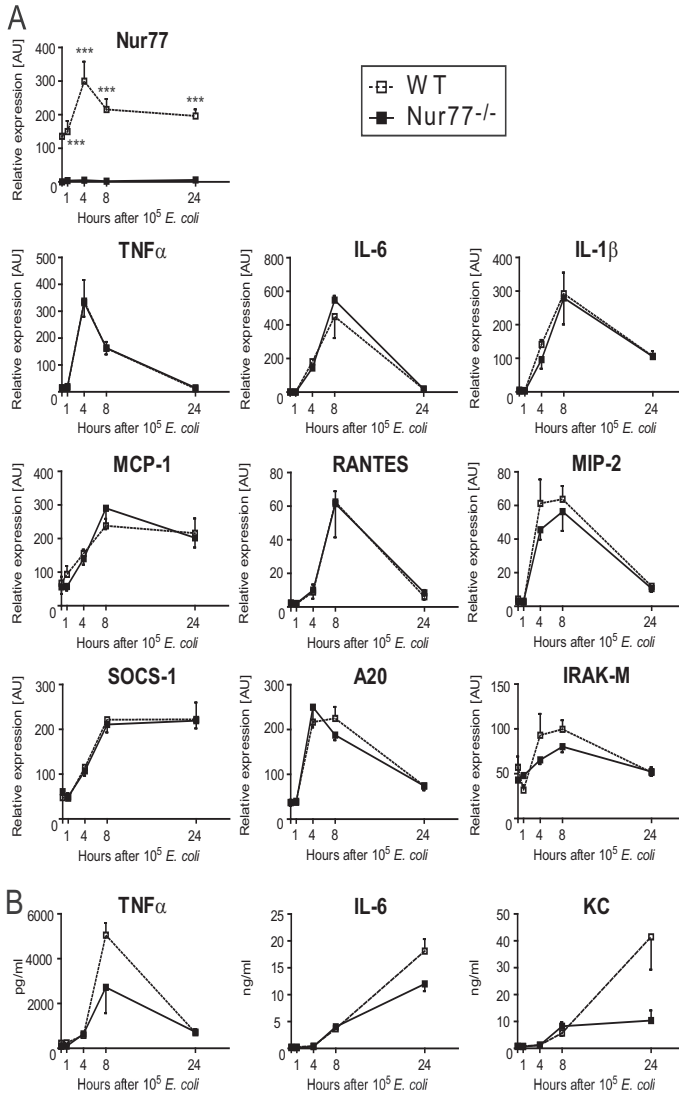
FIG 5 Expression of inflammatory genes and proteins by WT and Nur77$^{-/-}$ peritoneal macrophages in response to *E. coli*. Peritoneal macrophages were incubated with 10^5 growth-arrested *E. coli* bacteria, and at the indicated times, mRNA expression relative to 36B4 (A) and cytokine production (B) were evaluated. Data are means ± SEM ($n = 3$ mice/group) (∗∗∗, $P < 0.001$). AU, arbitrary units.

dothelial nitric oxide synthase (eNOS) mRNA levels after Nur77 overexpression, again indicating a role for Nur77 in endothelial barrier function. Western blots of HUVEC lysates showed that levels of ZO-1, VE-cadherin, occludin, claudin-5, and β-catenin were diminished after Nur77 overexpression, independent of *E. coli* stimulation (Fig. 7A and B). The P-eNOS/eNOS ratio was not changed after Nur77 overexpression (Fig. 7A and B). In order to visualize the junctions, we performed immunofluorescence for Nur77, VE-cadherin, and phalloidin on Nur77-overexpressing HUVECs and found VE-cadherin levels to be severely decreased on cells that stained

positive for Nur77 (Fig. 7C). The Nur77-induced loss of cell-cell junctions increased HUVEC monolayer permeability, as determined by transendothelial diffusion of FITC-dextran and resistance measurements using ECIS (Fig. 7). A significant increase in the transendothelial flux of fluorescent dextran was seen after Nur77 overexpression, and this was still apparent after *E. coli* stimulation (Fig. 7D). In addition, the transendothelial resistance of the Nur77-overexpressing monolayers was markedly decreased (39.1%) compared to that of control cells (Fig. 7E), emphasizing that Nur77 has a major effect on endothelial cell permeability.
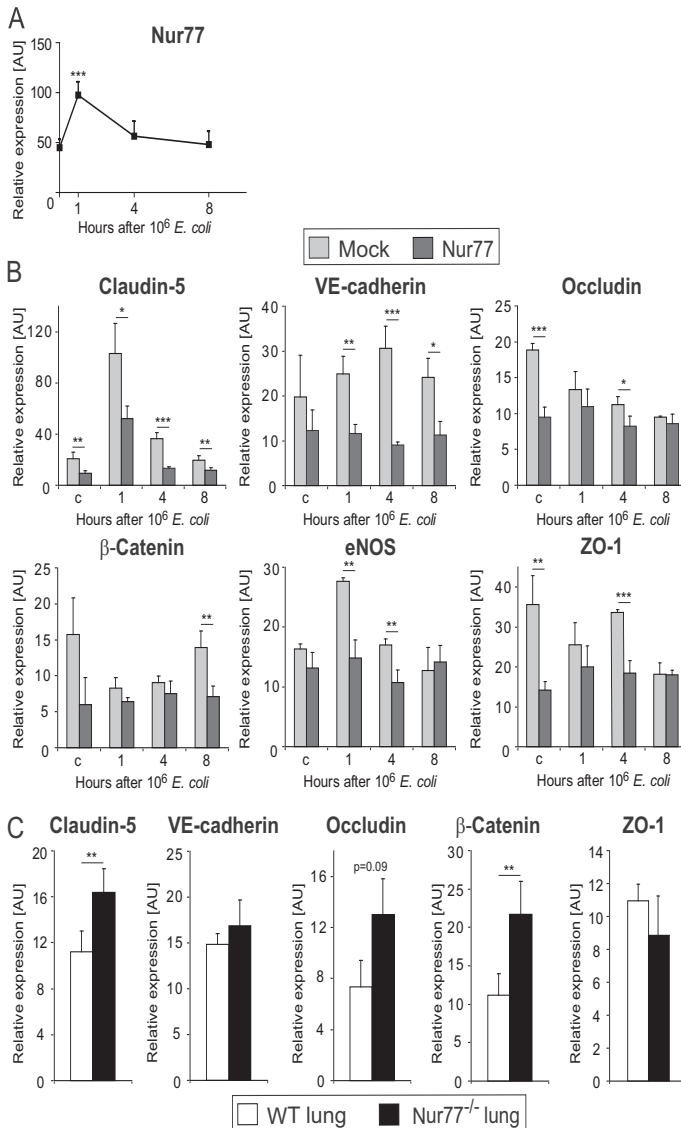
FIG 6 Role of Nur77 in endothelial cell tight and adherens junctions. (A and B) Human umbilical vein endothelial cells (HUVECs) were isolated and stimulated with 10^6 growth-arrested *E. coli* bacteria directly (A) or transduced with lentivirus encoding Nur77 or a control virus (Mock) prior to *E. coli* exposure (B). mRNA expression relative to 36B4 was evaluated. Data are representative of at least four independent experiments from different HUVEC isolations. (C) In addition, mRNA from WT and Nur77$^{-/-}$ healthy lungs was evaluated. Data represent 4 mice per group. Data are means $\pm$ SD ($*$, $P < 0.05$; $**$, $P < 0.01$; $***$, $P < 0.001$).

DISCUSSION

Nur77 is expressed in several immune cells, including macrophages and T cells, and in the endothelium [30, 31]. Most recently, it has been demonstrated that Nur77 has a crucial function in differentiation of Ly6C^{lo} monocytes, which are lacking in Nur77$^{-/-}$ mice [19]. This nuclear receptor plays a role in chronic inflammation conditions such as atherosclerosis [10, 16, 17] and rheumatoid arthritis [32]. Nurr1, another member of the NR4A subfamily, has also been implicated in several chronic inflammatory diseases, namely, psoriasis [33], inflammatory arthritis [34], and osteoarthritis [35]. Furthermore, all three NR4A subfamily members have been implicated in atopic dermatitis [36]. However, these nuclear receptors have never been studied in an acute bacterial infection model. In the present study, we describe our findings that provide insight into the role of Nur77 in Gram-negative infections such as peritonitis. *E. coli* is the most frequently found pathogen in the peritoneal fluid of peritonitis patients, namely, in 60% of the cases [3]. Therefore, we induced peritonitis
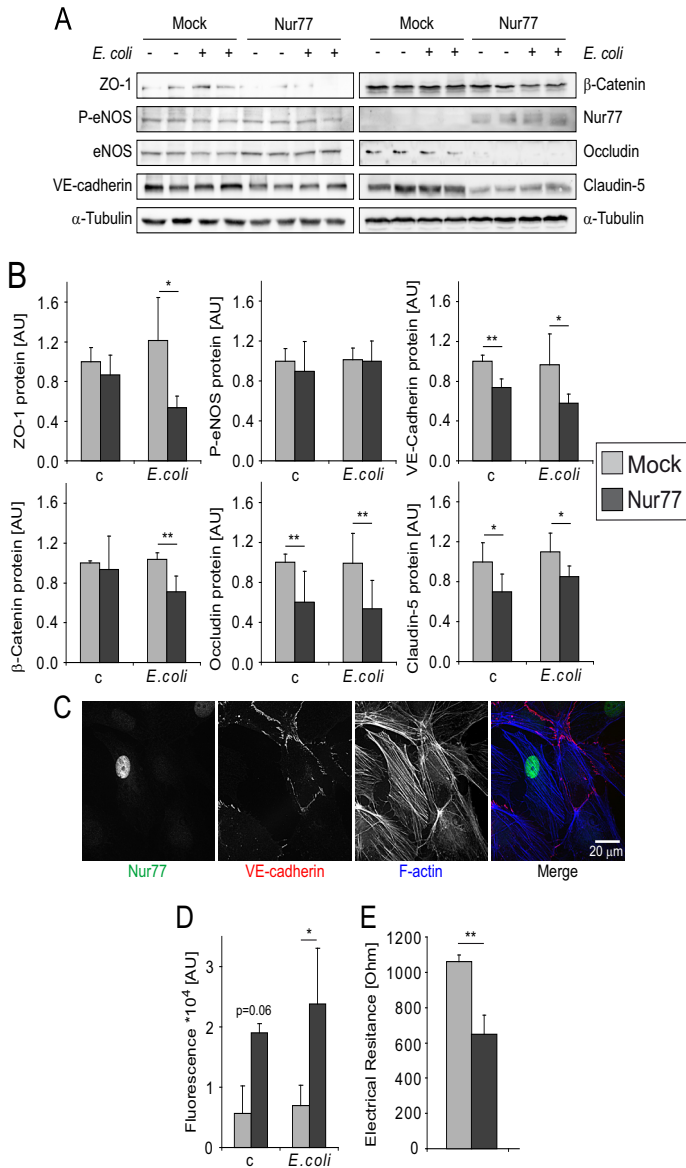
FIG 7 Functional role of Nur77 in endothelial cell permeability. HUVECs were isolated, transduced with lentivirus encoding Nur77 or a control virus (Mock), and stimulated with 10^6 growth-arrested *E. coli* bacteria. (A and B) Protein expression was evaluated by Western blotting (A), and band intensity was quantified by using ImageJ (B). All proteins were corrected for α-tubulin; only P-eNOS (Ser^{1177}) was corrected for total eNOS. Data from at least three independent experiments from different HUVEC isolations were combined in one graph ($n = 6$). (C) Combined immunofluorescence staining for Nur77 and VE-cadherin was performed on unstimulated Nur77-overexpressing HUVECs. (D and E) Permeability was evaluated by 40 min of transendothelial FITC-dextran (70 kDa) flux (D), and barrier function was evaluated by electric cell-substrate impedance sensing (ECIS) averaged over a period of 12 h (E). Data are means ± SD (∗, $P <$ 0.05; ∗∗, $P < 0.01$; ∗∗∗, $P < 0.001$).

by challenging mice with *E. coli* bacteria. We used an intraperitoneal *E. coli* dose of 10^4 CFU, which is the lowest inoculum that consistently results in sepsis in WT C57BL/6 mice (25).

In the current investigation, we did not find a role for Nur77 in host defense in the PLF and blood. These findings are substantiated by our differentials performed on cytospins of PLF showing no differences in monocytes, macrophages, or neutrophils. Inconsistent with the neutrophil numbers, there were changes in KC production found in the PLF of the Nur77$^{-/-}$ mice. Proinflammatory cytokines play an important role in the early response to

bacteria; therefore, we determined cytokine levels in the PLF and plasma. No difference was seen in TNF-α, IL-6, MCP-1, and IL-10 levels in these compartments of WT and Nur77$^{-/-}$ mice, whereas KC levels were lower in the PLF of Nur77$^{-/-}$ mice. During inflammation, E-selectin is expressed on endothelial cells and is eventually shed into the blood. Soluble E-selectin levels were slightly decreased in Nur77$^{-/-}$ plasma, indicating a possible effect on endothelial cell activation.

To investigate whether WT and Nur77$^{-/-}$ macrophages respond to these bacteria in a different manner, we cultured peritoneal macrophages and stimulated them with 10^5 growth-arrested *E. coli* bacteria. Again, no differences were found between WT and Nur77$^{-/-}$ macrophages in TNF-α, KC, and IL-6 production or in mRNA expression of several cytokines and chemokines known to be upregulated in this model. These results are not in agreement with data reported previously by our group and others, in which macrophages were stimulated with LPS (10, 16–18). One explanation may be that LPS is only one of a whole range of antigens present on *E. coli* bacteria. More specifically, LPS activates TLR4, whereas *E. coli* can also activate TLR2, -5, and -9 (21), leading to a difference in the inflammatory state of macrophages. Investigations using LPS as an inciting stimulus may therefore not adequately mimic Gram-negative infection, considering the above-mentioned complex composition of intact bacteria and the absence of a growing bacterial load.

Unlike our results for the PLF and blood compartment, we did find a transient minor but significantly increased bacterial clearance in the lung and liver compartments of Nur77$^{-/-}$ mice 14 h after inoculation. However, there were no differences found in the numbers of neutrophils in lungs and liver or macrophages present in the liver of these mice.

Nur77 is induced in endothelial cells by several stimuli, such as hypoxia, TNF-α, IL-1β, and vascular endothelial growth factor (VEGF) (27, 28). Stimulation of HUVECs with 10^6 growth-arrested *E. coli* bacteria resulted in increased Nur77 mRNA expression levels. Therefore, we investigated the influence of Nur77 on endothelial tight and adherens junctions in HUVECs and found that, in line with previous observations, claudin-5, VE-cadherin, and occludin expression levels were decreased after lentiviral overexpression of Nur77, indicating a role for Nur77 in vascular permeability (29). Downregulation of the tight junction proteins claudin-5, ZO-1, and occludin and the adherens junction proteins VE-cadherin and β-catenin upon Nur77 overexpression may explain the initially decreased bacterial load seen in the lungs and liver of Nur77$^{-/-}$ mice at 14 h postinfection. In addition, we showed increased mRNA expression levels of claudin-5, occludin, and β-catenin in the lungs of healthy Nur77$^{-/-}$ mice. Moreover, we found diminished TER and increased transendothelial dextran flux in Nur77-overexpressing HUVECs, pointing more toward an increased barrier function of the endothelium resulting in a lower bacterial load in the lungs/livers of Nur77$^{-/-}$ mice rather than the initially hypothesized increase in bacterial clearance.

The resulting tissue damage at 20 h postinfection was notably affected by Nur77 deficiency, especially in the liver. Liver necrosis was significantly lower in Nur77$^{-/-}$ mice, reflected by reduced pathology scores and ASAT/ALAT levels in plasma. This was most likely caused by the lower bacterial load observed 14 h after infection in the tissues of these mice than in the tissues of WT mice. Based on cleaved caspase-3 expression, less liver cell apoptosis was found as early as 6 h after inoculation in Nur77$^{-/-}$ mice. Indeed,

Nur77 is well known for its inducing role in apoptosis of multiple cell types (37–39), in particular during thymocyte selection (40). The effect of Nur77 on liver cell apoptosis in the context of hepatitis B virus infection has been described by Lee and colleagues (20). They showed that Nur77 was induced in hepatocytes expressing the hepatitis B virus X protein, which can play a role in Fas/FasL-mediated apoptosis in these infected cells. In addition, a study by Yeo et al. (41) indicated that Nur77 is required for regulation of Fas/FasL-induced apoptosis in liver cells. Of note, in Nur77$^{-/-}$ mouse lungs, the cleaved caspase-3 protein expression level was lower, indicating less apoptosis. This corresponds with data from a previous study performed on cadmium-induced apoptosis of lung cells (42). It was shown that cadmium treatment induces Nur77 expression, which in turn increases the number of apoptotic cells in the lung.

In summary, we have demonstrated a limited role for Nur77 in a murine model of *E. coli*-induced peritonitis. Nur77 appears to be involved mainly in increasing bacterial influx into the organs via modulation of vascular permeability, resulting in enhanced organ damage. Nur77 does not seem to play a role in the excessive inflammatory response of immune cells toward *E. coli*.

REFERENCES

1. **Wittmann DH, Schein M, Condon RE.** 1996. Management of secondary peritonitis. Ann. Surg. **224**:10–18. http://dx.doi.org/10.1097/00000658-199607000-00003.

2. **Hotchkiss RS, Karl IE.** 2003. The pathophysiology and treatment of sepsis. N. Engl. J. Med. **348**:138–150. http://dx.doi.org/10.1056/NEJMra021333.

3. **Fieren MW.** 2012. The local inflammatory responses to infection of the peritoneal cavity in humans: their regulation by cytokines, macrophages, and other leukocytes. Mediators Inflamm. **2012**:976241. http://dx.doi.org/10.1155/2012/976241.

4. **Wang MC, Tseng CC, Wu AB, Huang JJ, Sheu BS, Wu JJ.** 2009. Different roles of host and bacterial factors in Escherichia coli extraintestinal infections. Clin. Microbiol. Infect. **15**:372–379. http://dx.doi.org/10.1111/j.1469-0691.2009.02708.x.

5. **Tabas I, Glass CK.** 2013. Anti-inflammatory therapy in chronic disease: challenges and opportunities. Science **339**:166–172. http://dx.doi.org/10.1126/science.1230720.

6. **Bone RC.** 1996. Immunologic dissonance: a continuing evolution in our understanding of the systemic inflammatory response syndrome (SIRS) and the multiple organ dysfunction syndrome (MODS). Ann. Intern. Med. **125**:680–687. http://dx.doi.org/10.7326/0003-4819-125-8-199610150-00009.

7. **Van Der Poll T, Meijers JC.** 2010. Systemic inflammatory response syndrome and compensatory anti-inflammatory response syndrome in sepsis. J. Innate Immun. **2**:379–380. http://dx.doi.org/10.1159/000318190.

8. **Pols TW, Bonta PI, de Vries CJ.** 2007. NR4A nuclear orphan receptors: protective in vascular disease? Curr. Opin. Lipidol. **18**:515–520. http://dx.doi.org/10.1097/MOL.0b013e3282ef77d1.

9. **Zhao Y, Bruemmer D.** 2010. NR4A orphan nuclear receptors: transcriptional regulators of gene expression in metabolism and vascular biology. Arterioscler. Thromb. Vasc. Biol. **30**:1535–1541. http://dx.doi.org/10.1161/ATVBAHA.109.191163.

10. **Bonta PI, van Tiel CM, Vos M, Pols TW, van Thienen JV, Ferreira V, Arkenbout EK, Seppen J, Spek CA, Van Der Poll T, Pannekoek H, de Vries CJ.** 2006. Nuclear receptors Nur77, Nurr1, and NOR-1 expressed in

atherosclerotic lesion macrophages reduce lipid loading and inflammatory responses. Arterioscler. Thromb. Vasc. Biol. **26**:2288–2294. http://dx .doi.org/10.1161/01.ATV.0000238346.84458.5d.

11. **Pei L, Castrillo A, Chen M, Hoffmann A, Tontonoz P.** 2005. Induction of NR4A orphan nuclear receptor expression in macrophages in response to inflammatory stimuli. J. Biol. Chem. **280**:29256–29262. http://dx.doi .org/10.1074/jbc.M502606200.

12. **Shao Q, Shen LH, Hu LH, Pu J, Qi MY, Li WQ, Tian FJ, Jing Q, He B.** 2010. Nuclear receptor Nur77 suppresses inflammatory response dependent on COX-2 in macrophages induced by oxLDL. J. Mol. Cell. Cardiol. **49**:304–311. http://dx.doi.org/10.1016/j.yjmcc.2010.03.023.

13. **Pei L, Castrillo A, Tontonoz P.** 2006. Regulation of macrophage inflammatory gene expression by the orphan nuclear receptor Nur77. Mol. Endocrinol. **20**:786–794.

14. **Diatchenko L, Romanov S, Malinina I, Clarke J, Tchivilev I, Li X, Makarov SS.** 2005. Identification of novel mediators of NF-kappaB through genome-wide survey of monocyte adherence-induced genes. J. Leukoc. Biol. **78**:1366–1377. http://dx.doi.org/10.1189/jlb.0405211.

15. **Harant H, Lindley IJ.** 2004. Negative cross-talk between the human orphan nuclear receptor Nur77/NAK-1/TR3 and nuclear factor-kappaB. Nucleic Acids Res. **32**:5280–5290. http://dx.doi.org/10.1093/nar/gkh856.

16. **Hamers AA, Vos M, Rassam F, Marinkovic G, Kurakula K, van Gorp PJ, de Winther MP, Gijbels MJ, de Waard V, de Vries CJ.** 2012. Bone marrow-specific deficiency of nuclear receptor Nur77 enhances atherosclerosis. Circ. Res. **110**:428–438. http://dx.doi.org/10.1161 /CIRCRESAHA.111.260760.

17. **Hanna RN, Shaked I, Hubbeling HG, Punt JA, Wu R, Herrley E, Zaugg C, Pei H, Geissmann F, Ley K, Hedrick CC.** 2012. NR4A1 (Nur77) deletion polarizes macrophages toward an inflammatory phenotype and increases atherosclerosis. Circ. Res. **110**:416–427. http://dx.doi.org/10 .1161/CIRCRESAHA.111.253377.

18. **Chao LC, Soto E, Hong C, Ito A, Pei L, Chawla A, Conneely OM, Tangirala RK, Evans RM, Tontonoz P.** 2013. Bone marrow NR4A expression is not a dominant factor in the development of atherosclerosis or macrophage polarization in mice. J. Lipid Res. **54**:806–815. http://dx.doi .org/10.1194/jlr.M034157.

19. **Hanna RN, Carlin LM, Hubbeling HG, Nackiewicz D, Green AM, Punt JA, Geissmann F, Hedrick CC.** 2011. The transcription factor NR4A1 (Nur77) controls bone marrow differentiation and the survival of Ly6C⁻ monocytes. Nat. Immunol. **12**:778–785. http://dx.doi.org/10.1038/ni .2063.

20. **Lee MO, Kang HJ, Cho H, Shin EC, Park JH, Kim SJ.** 2001. Hepatitis B virus X protein induced expression of the Nur77 gene. Biochem. Biophys. Res. Commun. **288**:1162–1168. http://dx.doi.org/10.1006/bbrc.2001 .5910.

21. **van 't Veer C, van den Pangaart PS, Kruijswijk D, Florquin S, de Vos AF, Van Der Poll T.** 2011. Delineation of the role of Toll-like receptor signaling during peritonitis by a gradually growing pathogenic Escherichia coli. J. Biol. Chem. **286**:36603–36618. http://dx.doi.org/10.1074/jbc.M110 .189126.

22. **Jaffe EA, Nachman RL, Becker CG, Minick CR.** 1973. Culture of human endothelial cells derived from umbilical veins. Identification by morphologic and immunologic criteria. J. Clin. Invest. **52**:2745–2756.

23. **Fink MP, Heard SO.** 1990. Laboratory models of sepsis and septic shock. J. Surg. Res. **49**:186–196. http://dx.doi.org/10.1016/0022-4804(90)90260-9.

24. **Natanson C, Fink MP, Ballantyne HK, MacVittie TJ, Conklin JJ, Parrillo JE.** 1986. Gram-negative bacteremia produces both severe systolic and diastolic cardiac dysfunction in a canine model that simulates human septic shock. J. Clin. Invest. **78**:259–270. http://dx.doi.org/10.1172 /JCI112559.

25. **Sewnath ME, Olszyna DP, Birjmohun R, ten Kate FJ, Gouma DJ, van Der Poll T.** 2001. IL-10-deficient mice demonstrate multiple organ failure and increased mortality during Escherichia coli peritonitis despite an accelerated bacterial clearance. J. Immunol. **166**:6323–6331. http://www .jimmunol.org/content/166/10/6323.long.

26. **van Zoelen MA, Schmidt AM, Florquin S, Meijers JC, de Beer R, de Vos AF, Nawroth PP, Bierhaus A, Van Der Poll T.** 2009. Receptor for advanced glycation end products facilitates host defense during Esche-

richia coli-induced abdominal sepsis in mice. J. Infect. Dis. **200**:765–773. http://dx.doi.org/10.1086/604730.

27. **Liu D, Jia H, Holmes DI, Stannard A, Zachary I.** 2003. Vascular endothelial growth factor-regulated gene expression in endothelial cells: KDR-mediated induction of Egr3 and the related nuclear receptors Nur77, Nurr1, and Nor1. Arterioscler. Thromb. Vasc. Biol. **23**:2002–2007. http://dx.doi.org/10.1161/01.ATV.0000098644.03153.6F.

28. **Zeng H, Qin L, Zhao D, Tan X, Manseau EJ, Van Hoang M, Senger DR, Brown LF, Nagy JA, Dvorak HF.** 2006. Orphan nuclear receptor TR3/ Nur77 regulates VEGF-A-induced angiogenesis through its transcriptional activity. J. Exp. Med. **203**:719–729. http://dx.doi.org/10.1084/jem .20051523.

29. **Zhao D, Qin L, Bourbon PM, James L, Dvorak HF, Zeng H.** 2011. Orphan nuclear transcription factor TR3/Nur77 regulates microvessel permeability by targeting endothelial nitric oxide synthase and destabilizing endothelial junctions. Proc. Natl. Acad. Sci. U. S. A. **108**:12066–12071. http://dx.doi.org/10.1073/pnas.1018438108.

30. **Bandukwala HS, Rao A.** 2013. 'Nurr'ishing Treg cells: Nr4a transcription factors control Foxp3 expression. Nat. Immunol. **14**:201–203. http://dx .doi.org/10.1038/ni.2546.

31. **van Tiel CM, de Vries CJ.** 2012. NR4All in the vessel wall. J. Steroid Biochem. Mol. Biol. **130**:186–193. http://dx.doi.org/10.1016/j.jsbmb .2011.01.010.

32. **de Silva S, Han S, Zhang X, Huston DP, Winoto A, Zheng B.** 2005. Reduction of the incidence and severity of collagen-induced arthritis by constitutive Nur77 expression in the T cell lineage. Arthritis Rheum. **52**: 333–338. http://dx.doi.org/10.1002/art.20736.

33. **O'Kane M, Markham T, McEvoy AN, Fearon U, Veale DJ, FitzGerald O, Kirby B, Murphy EP.** 2008. Increased expression of the orphan nuclear receptor NURR1 in psoriasis and modulation following TNF-alpha inhibition. J. Invest. Dermatol. **128**:300–310. http://dx.doi.org/10.1038/sj .jid.5701023.

34. **Aherne CM, McMorrow J, Kane D, FitzGerald O, Mix KS, Murphy EP.** 2009. Identification of NR4A2 as a transcriptional activator of IL-8 expression in human inflammatory arthritis. Mol. Immunol. **46**:3345–3357. http://dx.doi.org/10.1016/j.molimm.2009.07.019.

35. **Ralph JA, McEvoy AN, Kane D, Bresnihan B, FitzGerald O, Murphy EP.** 2005. Modulation of orphan nuclear receptor NURR1 expression by methotrexate in human inflammatory joint disease involves adenosine A2A receptor-mediated responses. J. Immunol. **175**:555–565. http://www .jimmunol.org/content/175/1/555.long.

36. **Kagaya S, Hashida R, Ohkura N, Tsukada T, Sugita Y, Terakawa M, Tsujimoto G, Katsunuma T, Akasawa A, Matsumoto K, Saito H.** 2005. NR4A orphan nuclear receptor family in peripheral blood eosinophils from patients with atopic dermatitis and apoptotic eosinophils in vitro. Int. Arch. Allergy Immunol. **137**(Suppl 1):35–44. http://dx.doi.org/10 .1159/000085430.

37. **Kim SO, Ono K, Tobias PS, Han J.** 2003. Orphan nuclear receptor Nur77 is involved in caspase-independent macrophage cell death. J. Exp. Med. **197**:1441–1452. http://dx.doi.org/10.1084/jem.20021842.

38. **Li Y, Lin B, Agadir A, Liu R, Dawson MI, Reed JC, Fontana JA, Bost F, Hobbs PD, Zheng Y, Chen GQ, Shroot B, Mercola D, Zhang XK.** 1998. Molecular determinants of AHPN (CD437)-induced growth arrest and apoptosis in human lung cancer cell lines. Mol. Cell. Biol. **18**:4719–4731.

39. **Wilson AJ, Arango D, Mariadason JM, Heerdt BG, Augenlicht LH.** 2003. TR3/Nur77 in colon cancer cell apoptosis. Cancer Res. **63**:5401–5407. http://cancerres.aacrjournals.org/content/63/17/5401.long.

40. **Dequiedt F, Kasler H, Fischle W, Kiermer V, Weinstein M, Herndier BG, Verdin E.** 2003. HDAC7, a thymus-specific class II histone deacetylase, regulates Nur77 transcription and TCR-mediated apoptosis. Immunity **18**:687–698. http://dx.doi.org/10.1016/S1074-7613(03)00109-2.

41. **Yeo MG, Yoo YG, Choi HS, Pak YK, Lee MO.** 2005. Negative cross-talk between Nur77 and small heterodimer partner and its role in apoptotic cell death of hepatoma cells. Mol. Endocrinol. **19**:950–963. http://dx.doi .org/10.1210/me.2004-0209.

42. **Shin HJ, Lee BH, Yeo MG, Oh SH, Park JD, Park KK, Chung JH, Moon CK, Lee MO.** 2004. Induction of orphan nuclear receptor Nur77 gene expression and its role in cadmium-induced apoptosis in lung. Carcinogenesis **25**:1467–1475. http://dx.doi.org/10.1093/carcin/bgh135.